Progress In Electromagnetics Research B, Vol. 51, 119–133, 2013

ELECTROMAGNETIC TOPOLOGY ANALYSIS OF EXTERNAL PULSES INTERACTION WITH SHIELDED CABLES USING SPICE MODELS

Haiyan Xie*, Jianguo Wang, Yong Li, Shuang Li, Chun Xuan, and Yue Wang

Northwest Institute of Nuclear Technology, P. O. Box 69-12, Xi'an, Shanxi 710024, China

Abstract—Simulations based on electromagnetic topology (EMT) have been carried out to analyze an external electromagnetic pulse interaction with a shielded coaxial cable linking two systems together. The proposed EMT approach, combined with the SPICE model of the shielded cable, can be applied in the transient simulation directly and used for the electromagnetic interference analysis of systems including nonlinear devices. The effects of the outer terminators, cable length, and connection of the voltage limiter on the induced voltages at the systems are studied by using the proposed EMT approach. It has been found that adding a resistance between the system's shielding enclosure and the ground can effectively reduce the coupling through the shielded cable. The cable length affects the pulse-widths rather than the magnitudes of the induced voltages. The results also show that the voltage limiter can reduce the induced voltages but at the same time result in mismatch at the source or load.

1. INTRODUCTION

The process through which external electromagnetic pulses (EMPs) couple into the electronic systems and generate interferences on inner circuits or devices is an important problem for system design. However, it is complicated due to several issues below. First, external electromagnetic fields can couple into systems through various paths, such as antennas, apertures or slits on shielding enclosure, and power or data lines. Second, systems comprise different types of structures, for example, cavities, cables, integrated circuits, and semiconductor

Received 10 March 2013, Accepted 8 April 2013, Scheduled 23 April 2013

* Corresponding author: Haiyan Xie (xiehy05@foxmail.com).

devices. These structures can have different governing equations. At last, electronic systems usually have nonlinear protection devices, and the intense electromagnetic fields of external pulses may generate nonlinear effects (such as damage) on the systems. Consequently, physics of the interaction process is difficult to follow.

It is difficult to analyze such a complicated process by using a single method. Three-dimensional (3-D) numerical methods, such as finite difference time domain (FDTD) method, require discretization of the whole geometry. As a result, these methods need colossal computation time and large memory due to very small mesh spacing corresponding to the tiniest dimension in the geometry. Physics of the process may be lost in the huge amount of data generated. Moreover, the 3-D electromagnetic (EM) numerical methods can only be suitable for the EM problems, such as the analyses of antennas, cavities, and apertures, but electronic systems also consist of cables, integrated circuits, semiconductor devices, and so on. Analyzing the process via experiment is a straightforward approach. The experimental approach is usually employed to obtain the thresholds of devices. However, for a whole complicated system, it costs a lot and needs a long term. Moreover, only limited experimental data at limited places can be obtained, which is inadequate for the analysis of the whole system [1]. As a result, it is difficult to understand the physics of the process only through experiments.

To analyze the complicated process, the electromagnetic topology (EMT) method was proposed in the early 1980s [2, 3]. At first, it was used as a system design methodology for formalizing the design of electrical systems to withstand the effects of various EM threats [4]. Afterwards, with the efforts of many researchers [5–7], it became a simulation tool for the prediction of EM interferences generated by external EM threats on systems [8–12]. In the EMT method, electronic systems can be decomposed into manageable sizes of sub-volumes which can be modeled by different methods, numerically or experimentally. These sub-volumes do not interact with each other except through preferred paths, typically, cables and apertures. The sub-volumes are treated as junctions, the interaction paths among the sub-volumes are treated as tubes, and then a network equation, the Baum-Liu-Tesche (BLT) equation [5], can be established. However, junctions in the BLT equation are treated as black boxes and are described by the scattering parameter, which implies that junctions should be linear. Actually, there are many nonlinear devices in systems and the effects generated by external pulses can be nonlinear. To solve this problem, the SPICE model of multiconductor transmission line was proposed in the EMT approach [13, 14]. The proposed method

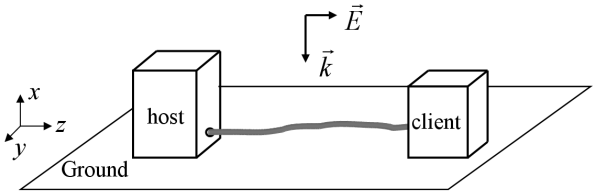

Figure 1. The external pulse interaction with a shielded cable connecting two systems.

has been employed to study EMP coupling to a system through a wire and good agreement with experimental results has been obtained [15]. Then the SPICE model for shielded cable has also been developed [16] and has been applied in the EMT approach, which has been validated against the experiment [17].

In this paper, external EMP interaction with a shielded cable connecting two systems, as shown in Figure 1, is studied by using a new EMT approach which employs a SPICE model of the shielded cable [16]. The study can be applied to the interference analysis of external electromagnetic pulse on real-life electronic systems which are always linked together to exchange data. The new EMT approach is also introduced and has the advantage for the interference analysis of nonlinear systems compared with the conventional one. With this approach, the influences of the outer terminal loads, cable length, and nonlinear protection devices at the ports on the EM interferences generated by an external pulse are investigated. In Section 2, a brief description of the interaction process is provided while Section 3 introduces the EMT approach using the SPICE model of the shielded cable to the simulation process. Results and discussions are given in Section 4 and we conclude in Section 5.

2. THE INTERACTION PROCESS DESCRIPTION

Figure 1 shows a shielded coaxial cable connecting a client with a host located over a perfectly conducting ground illuminated by an external electromagnetic pulse. The cable shield is connected to the shielding enclosures of the host and the client at the ends directly, while the inner wire of the cable links the devices of the host and the client which are denoted by the resistances R_1 and R_2, respectively, as shown in Figure 2. The enclosures of the host and the client are connected to the ground plane by external resistances R_{out1} and R_{out2}, respectively. To protect the devices from external disturbances, nonlinear protection

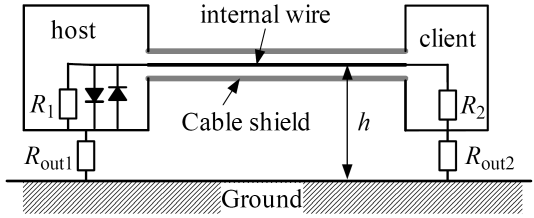

Figure 2. The connection configuration.

devices (voltage limiters here) are always connected to the devices in parallel.

The surface of the cable shield's outer layer and shielding enclosures make up the shielding of the whole configuration. The external electromagnetic pulse can induce currents and charges on the shielding. When the height of the shielded cable over the ground is electrically small compared with the wavelength, the exterior of the cable shield and the ground can constitute a transmission-line system with the loads R_{out1} and R_{out2} as its terminators. Then a cable shield current and a shield-to-ground voltage (or equivalently, a shield charge density) will be generated by the external pulse.

However, the shielding composed of the cable shield and shielding enclosures is not perfect. The electric and magnetic fields of external pulses can penetrate through the imperfections in the cable shield and give rise to disturbing currents and voltages on the internal wire. Then these disturbances can propagate along the internal wire to the terminal devices inside the host and the client, and generate interferences on them.

The coupling between the external electromagnetic fields and the internal wire of the shielded cable is a complex process. It happens mainly in three manners, fields diffusing through the shield material, fields penetrating through the small apertures on the shield, and the induction due to overlapping of the individual strands of the shield [18, 19]. However, the coupling effect can be described in terms of the transfer impedance Z_t and the transfer admittance Y_t of the shield, which describe the processes by which a portion of the induced current and the induced charge on the shield find their way onto the internal wire, respectively. And these result in a distributed voltage source between the internal wire and the shield and a distributed current source injected on the internal wire, respectively. These distributed voltage and current sources will yield interferences on the devices at the termination of the inner transmission-line which is composed of interior of the cable shield and the internal wire.

3. SIMULATION APPROACH FOR THE INTERACTION PROCESS

With the coupling process described as above, the induced voltage and current of the outer transmission-line system composed of the shield's exterior and the ground should be determined first. Due to the good shielding of the shield, the energy transferred from the inner system to the outer system through the shield can be neglected. Then the coupling of external fields with the outer transmission-line system can be described through Taylor's formulation [20] and the induced voltage V_{out} and current I_{out} can be solved from the equation

$$\begin{aligned} \frac{\partial}{\partial z}V_{\text{out}}(z,t) + L_{\text{out}}\frac{\partial}{\partial t}I_{\text{out}}(z,t) &= V_{F\text{out}}(z,t) \\ \frac{\partial}{\partial z}I_{\text{out}}(z,t) + C_{\text{out}}\frac{\partial}{\partial t}V_{\text{out}}(z,t) &= I_{F\text{out}}(z,t) \end{aligned}. \tag{1}$$

Here L_{out} and C_{out} are the per-unit-length (p.u.l.) inductance and capacitance of the outer transmission-line system, respectively. $V_{F_{\text{out}}}$ and $I_{F_{\text{out}}}$ are the distributed voltage and current sources due to the excitation fields and they can be expressed by the following equations

$$\begin{aligned} V_{F\text{out}}(z,t) &= -\frac{\partial}{\partial z}E_T(z,t) + E_L(z,t) \\ I_{F\text{out}}(z,t) &= -C_{\text{out}}\frac{\partial}{\partial t}E_T(z,t) \end{aligned}, \tag{2}$$

where

$$\begin{aligned} E_T(z,t) &= \int_0^h E_x^{ex}(x,z,t)\,dx \\ E_L(z,t) &= E_z^{ex}(h,z,t) \end{aligned}. \tag{3}$$

E_x^{ex} and E_z^{ex} are the components of excitation electric field along the x and z axes, respectively. Due to the scattering of the shielding enclosures of the systems and the reflection of the ground, the excitation electric field E^{ex} is different from the incident electric field and a numerical method, such as the finite-difference time-domain (FDTD) method, can be utilized to compute the excitation field.

According to the interaction process, the voltage V_{in} and current I_{in} of the inner transmission-line system can be described by

$$\begin{aligned} \frac{\partial}{\partial z}V_{\text{in}}(z,t) + L_{\text{in}}\frac{\partial}{\partial t}I_{\text{in}}(z,t) &= V_{F\text{in}}(z,t) \\ \frac{\partial}{\partial z}I_{\text{in}}(z,t) + C_{\text{in}}\frac{\partial}{\partial t}V_{\text{in}}(z,t) &= I_{F\text{in}}(z,t) \end{aligned}, \tag{4}$$

where L_{in} and C_{in} are the p.u.l. inductance and capacitance of the inner transmission-line system. $V_{F\text{in}}$ and $I_{F\text{in}}$ are the distributed voltage and current sources, respectively, and they can be expressed in terms of the transfer impedance Z_t and admittance Y_t as

$$\begin{aligned} V_{F\text{in}} &= Z_{\text{t}}(t) * I_{\text{out}}(z,t) \\ I_{F\text{in}} &= -Y_{\text{t}}(t) * V_{\text{out}}(z,t) \end{aligned}. \tag{5}$$

Here the operator '*' denotes the convolution computation. With Equations (1) and (4) the relations between the terminal voltages and currents of the two transmission-line systems can be expressed as [16, 21]

$$\begin{aligned} & V_{\text{out}}(0,t) - Z_{C\text{out}} I_{\text{out}}(0,t) \\ =& V_{\text{out}}(l, t - T_{\text{out}}) - Z_{C\text{out}} I_{\text{out}}(l, t - T_{\text{out}}) + V_{0\text{out}}(t) \\ & V_{\text{out}}(l,t) + Z_{C\text{out}} I_{\text{out}}(l,t) \\ =& V_{\text{out}}(0, t - T_{\text{out}}) + Z_{C\text{out}} I_{\text{out}}(0, t - T_{\text{out}}) + V_{l\text{out}}(t) \end{aligned} \tag{6}$$

$$\begin{aligned} & V_{\text{in}}(0,t) - Z_{C\text{in}} I_{\text{in}}(0,t) \\ =& V_{\text{in}}(l, t - T_{\text{in}}) - Z_{C\text{in}} I_{\text{in}}(l, t - T_{\text{in}}) + V_{0\text{in}}(t) \\ & V_{\text{in}}(l,t) + Z_{C\text{in}} I_{\text{in}}(l,t) \\ =& V_{\text{in}}(0, t - T_{\text{in}}) + Z_{C\text{in}} I_{\text{in}}(0, t - T_{\text{in}}) + V_{l\text{in}}(t). \end{aligned} \tag{7}$$

Here $Z_{C\text{out}}$, T_{out} and $Z_{C\text{in}}$, T_{in} are the characteristic impedances and one-way time delays of the outer and inner transmission-line systems, respectively. l is the length of the shielded cable. $V_{0\text{out}}$ and $V_{l\text{out}}$ are total forcing functions representing the effect of excitation field on the outer system and are given by

$$\begin{aligned} V_{0\text{out}}(t) &= -\int_0^l E_L(z, t - z/v_{\text{out}})dz + E_T(l, t - T_{\text{out}}) - E_T(0,t) \\ V_{l\text{out}}(t) &= \int_0^l E_L(z, t - T_{\text{out}} + z/v_{\text{out}})dz - E_T(l,t) + E_T(0, t - T_{\text{out}}) \end{aligned}, \tag{8}$$

where ν_{out} is the wave propagation velocity of the outer transmission-line system. $V_{0\text{out}}$ and $V_{l\text{out}}$ can be calculated by using the numerical integration method [23] and incorporated into the SPICE circuit of the shielded cable as independent voltage sources. $V_{0\text{in}}$ and $V_{l\text{in}}$ are total forcing functions of the inner system, which denote the coupling effects of excitation fields on the inner system, and they are given by

$$\begin{aligned} V_{0\text{in}}(t) &= -\int_0^l [V_{F\text{in}}(z, t - z/v_{\text{in}}) - Z_{C\text{in}} I_{F\text{in}}(z, t - z/v_{\text{in}})]dz \\ V_{l\text{in}}(t) &= \int_0^l [V_{F\text{in}}(z, t - T_{\text{in}} + z/v_{\text{in}}) + Z_{C\text{in}} I_{F\text{in}}(z, t - T_{\text{in}} + z/v_{\text{in}})]dz \end{aligned}. \tag{9}$$

Here ν_{in} is the wave propagation velocity of the inner transmission-line system. $V_{0\text{in}}$ and $V_{l\text{in}}$ can be realized through delay lines, controlled

sources, and differential circuits in the SPICE circuit [16]. As a result, the configuration of the SPICE circuit for the coaxial shielded cable is shown in Figure 3.

Once the terminal connection configuration in Figure 2 is defined, the induced voltages and currents on the devices by the external pulse can be computed by using a SPICE software. Since the whole computation is carried out in the time domain, nonlinear terminators are allowed.

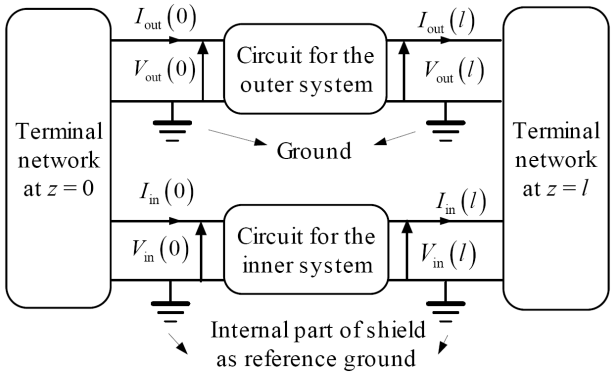

Figure 3. The structure of the SPICE model for the shielded cable excited by external fields.

4. RESULTS AND DISCUSSIONS

In our simulation, an EMP described by a biexponential pulse $E(t) = kE_0[\exp(-\beta t) - \exp(-\alpha t)]$, where $k = 1.3$, $E_0 = 50\,\mathrm{kV/m}$, $\alpha = 6.0 \times 10^8\,\mathrm{s}^{-1}$, and $\beta = 4.0 \times 10^7\,\mathrm{s}^{-1}$ [22], is employed as the source of external electromagnetic perturbation. The waveform and spectrum of the electric field of the EMP is shown in Figure 4. The client is connected to the host with a RG 58 shielded cable of which the characteristic impedance is $50\,\Omega$, and the relative dielectric constant of the inner medium is 1.85. Other parameters for the configuration are given in Table 1. The excitation fields at the cable are computed with a numerical FDTD code first, and then the induced voltages at the internal loads R_1 and R_2 are calculated with the SPICE circuit for the shielded cable where the excitation fields are incorporated as sources. The effects of the outer loads (R_{out1}, R_{out2}), the cable length, and the voltage limiters on the interferences caused by the external EMP are studied.

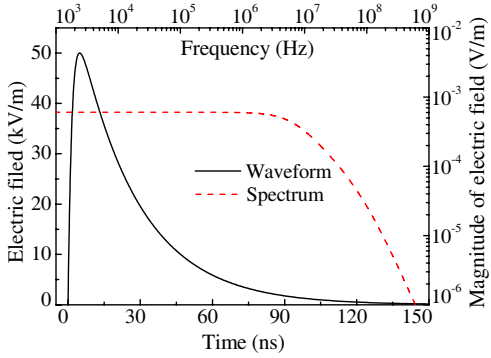

Figure 4. The waveform and spectrum of the electric filed of the EMP.

Table 1. Parameters for the configuration.

Parameters	Values
The enclosure dimension of the host	0.6 m × 0.4 m × 0.4 m
The enclosure dimension of the client	0.5 m × 0.3 m × 0.4 m
Inner loads R_1, R_2	50 Ω
Outer loads R_{out1}, R_{out2}	0 Ω, 100 Ω, 220.24 Ω, 500 Ω, 100 MΩ
Cable height h	3 cm
Cable length l	2 m, 5 m, 10 m
Number of voltage limiters	0, 1, 2

Figure 5 shows the induced voltages at the internal loads R_1 and R_2 generated by the EMP when the outer terminal loads ($R_{out1} = R_{out2}$) have different values, where the cable length l is 2 m and there is no voltage limiters at the connection ports. Five different values of the outer loads have been considered. The results show that the induced voltages are largest when the outer loads are 0 Ω which is the case when the shielding enclosures are connected to the ground directly. However, this is the most common case in reality. When the outer termination is matched, that is, the outer loads equal the characteristic impedance (220.24 Ω here) of the outer transmission-line system, the induced voltages are not the smallest but decay most

quickly. This is because other values of the outer terminators result in reflections at the ends of the outer system and the reflected voltage and current of the outer system can couple into the inner system and generate interferences, even though the inner transmission-line system is matched at both ends. To demonstrate the validity of the proposed method, the results obtained via the conventional EMT method when the outer termination is matched are also given, where the cable loss has been considered.

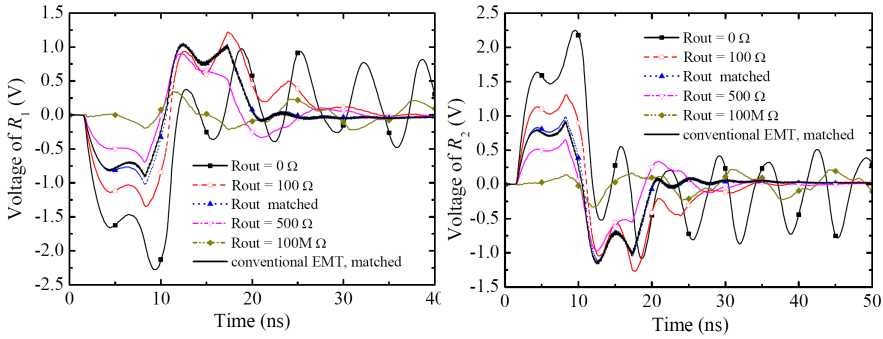

Figure 5. The induced voltages at the inner terminal loads as the functions of the outer terminal loads R_{out} (0 Ω, 100 Ω, matched, 500 Ω, and 100 MΩ) when the cable length is 2 m and the number of voltage limiters is 0. (a) The induced voltage of R_1. (b) The induced voltage of R_2.

The results also imply that the larger the outer loads are the smaller the induced voltage is. Both the shield current and shield charge contribute to the induced voltages at the internal loads. Figure 6 and Figure 7 show the induced voltages and currents at the outer loads R_{out1} and R_{out2}, respectively. The results show that the larger the outer loads the larger the shield-to-ground voltages but the smaller the shield currents. It can be concluded that the shield currents play a dominant role in the coupling onto the internal wire compared with the shield-to-ground voltages. According to [18] and [19], the transfer impedance and admittance of the shield can be expressed in the frequency domain as

$$\begin{matrix} \hat{Z}_t = R_{\text{dc}} + j\omega L_t \\ \hat{Y}_t = j\omega C_t \end{matrix}, \tag{10}$$

where R_{dc}, L_t, and C_t are the p.u.l. transfer resistance, inductance, and capacitance of the shield. For this configuration, it can be calculated

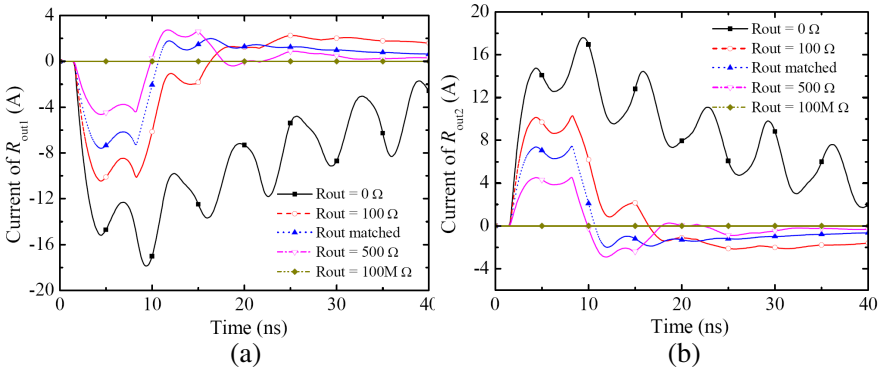

Figure 6. The voltages at the outer loads as the functions of the outer terminal loads R_{out} (0 Ω, 100 Ω, matched, 500 Ω, and 100 MΩ) when the cable length is 2 m and the number of voltage limiters is 0. (a) The voltages of R_{out1}. (b) The voltages of R_{out2}.

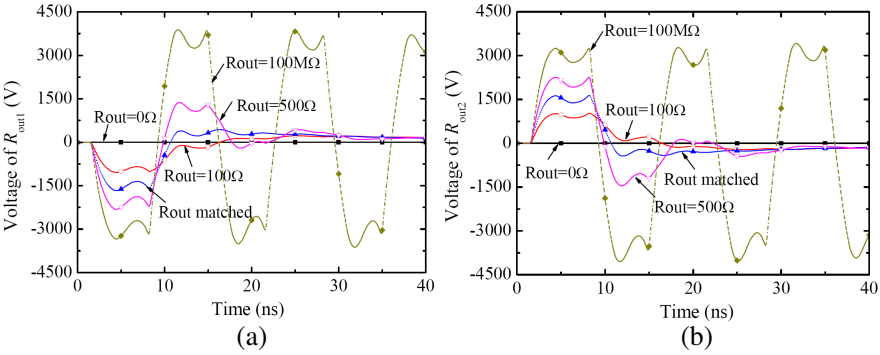

Figure 7. The currents of the outer loads as the functions of the outer terminal loads R_{out} (0 Ω, 100 Ω, matched, 500 Ω, and 100 MΩ) when the cable length is 2 m and the number of voltage limiters is 0. (a) The currents of R_{out1}. (b) The currents of R_{out2}.

that the transfer resistance R_{dc}, the transfer inductance L_t, and the transfer capacitance C_t are 14.2 mΩ/m, 1.0 nH/m, and 0.0639 pF/m, respectively. At the frequencies of interest, the transfer impedance is much larger than the transfer admittance, and this is because the electric field shielding of the shield is much better than the magnetic field shielding, which means that the shield current is more important than the shield-to-ground voltage for the induced voltage of the load R_1. As a result, in order to reduce the interferences on the device

generated by external pulses, one should add a resistance between the shielding enclosure and the ground rather than connect the enclosure to the ground directly.

Figure 8 shows the induced voltages at the inner loads R_1 and R_2 due to the external EMP changing with the cable length l when the outer termination is matched and no voltage limiters is connected to the termination. The results reveal that the increase of the cable length does not result in the magnitude increase of the induced voltages appreciable but broadens the pulse widths of the interferences. And the pulse widths of the induced voltages are directly and linearly proportional to the cable length. This is because the longer the cable the more voltage and current sources induced on cable according to the Equations (1) and (4); however, the effects of these excitation sources do not add up together to increase the magnitudes but widen the widths of the induced voltages due to the different time needed by these sources propagating to the terminal loads.

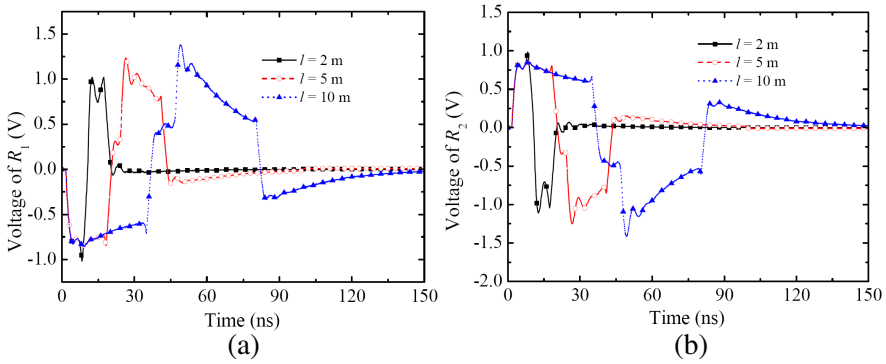

Figure 8. The induced voltages at the inner terminal loads as the functions of the cable length l (2, 5, and 10 m) when the outer loads R_{out1} and R_{out2} are matched and the number of voltage limiters is 0. (a) The induced voltage of R_1. (b) The induced voltage of R_2.

Electronic systems usually have nonlinear protection devices to protect them from external disturbances. In this paper, a voltage limiter, which is composed of two anti-parallel 1N4148 diodes, is considered and its effect is studied, as shown in Figure 2. Three cases, no voltage limiters (the first case), a voltage limiter connected in parallel to the loads R_1 shown in Figure 2 (the second case), and two voltage limiters connected to the loads R_1 and R_2 separately (the third case), are investigated by using the proposed EMT approach which applies the SPICE model for the shielded cable. Figures 9(a) and (b)

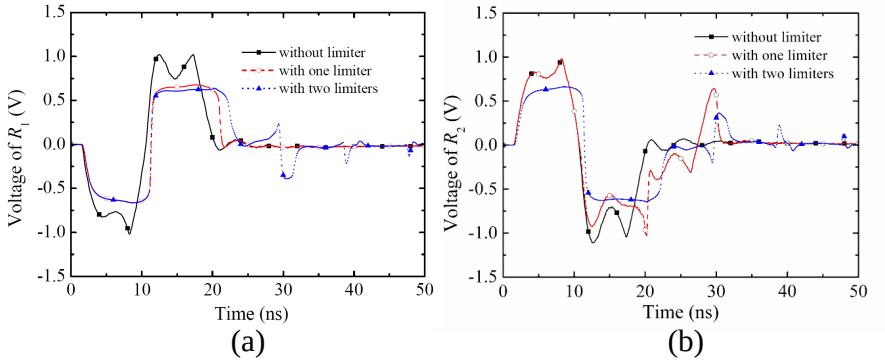

Figure 9. The induced voltages at the inner terminal loads as the functions of the voltage limiter number (0, 1, and 2) when the outer loads R_{out1} and R_{out2} are matched and the cable length is 2 m. (a) The induced voltage of R_1. (b) The induced voltage of R_2.

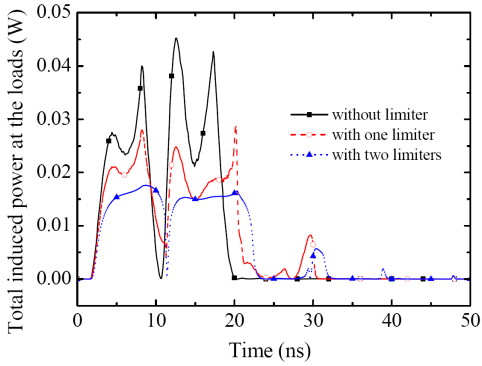

Figure 10. The total induced power at the inner terminal loads R_1 and R_2 as the functions of the voltage limiter number (0, 1, and 2) when the outer loads R_{out1} and R_{out2} are matched and the cable length is 2 m.

show the induced voltage at the loads R_1 and R_2 for the three cases, respectively. It can be concluded from the results that the voltage limiter can effectively limit the magnitudes of the induced voltages at the loads. As a result, the total induced power and energy at the both loads R_1 and R_2 decrease accordingly, as shown in Figure 10. However, the voltage limiter may increase the pulse width of the induced voltage at the load to which the limiter is connected. This is because the energy coupled onto the load needs more time to decay due to the decrease

of the induced power. The results also reveal that the voltage limiter introduces reflections on the induced voltages and the third case has more reflections than the second case. The reason for this is that the diode which makes up of the limiter has a small dynamic resistance when it works at conducting state [24], and this dynamic resistance makes the termination not match any more and results in a negative reflection coefficient at the end. The second case only has the voltage limiter at the near end while the third case has voltage limiters at both ends, which means only the near end is not matched in the second case, while both ends are not matched in the third case.

5. CONCLUSIONS

An external EMP interaction with a shielded coaxial cable, which links two systems together, has been studied by using a new EMT approach. It requires the determination of the excitation fields on the shielded cable first, and then a SPICE model for the shielded cable is employed to describe the coupling of the excitation fields with the shielded cable. The new EMT approach, which combines the SPICE model, can be utilized directly in the transient simulation and has the advantage for the electromagnetic interference analysis of nonlinear systems. The responses of the configuration to the external EMP changing with the outer termination, the cable length, and the connection of voltage limiters have been studied with the proposed EMT approach. The results show that the induced voltages are the largest when the shielding enclosure is connected to the ground directly, which is the most common case actually, and adding a resistance between the enclosure and the ground can reduce the induced voltages effectively. The analysis also shows that the cable length does not affect the magnitude of the induced voltage very much but the pulse-width of the induced voltage, which increases with the cable length nearly linearly. At last, it can be concluded from the results that the voltage limiter can limit effectively the magnitude of the induced voltage and reduce the power coupled to the devices; however, it can introduce mismatch at the source or load at the same time which will result in the reflections of the interferences and signals.

ACKNOWLEDGMENT

Acknowledgement is made to National Natural Science Foundation of China for the support of this work through Grant No. 61201090 and No. 61231003.

REFERENCES

1. Backstrom, M. G. and K. G. Lovstrand, "Susceptibility of electronic systems to high-power microwaves: Summary of test experience," *IEEE Trans. Electromagn. Compat.*, Vol. 46. No. 3, 396–403, 2004.
2. Tesche, F. M., "Topological concepts for internal EMP interaction," *IEEE Trans. Antennas. Propag.*, Vol. 26, No. 1, 60–64, 1978.
3. Baum, C. E., "Electromagnetic topology: A formal approach to the analysis and design of complex electronic systems," Interaction Notes, Note 400, 1980.
4. Lee, K. S. H., *EMP Interaction: Principles, Techniques and Reference Data*, EMP Interaction 2-1, 1986.
5. Baum, C. E., T. K. Liu, and F. M. Tesche, "On the analysis of general multiconductor transmission-line networks," Interaction Notes, Note 350, 1978.
6. Parmantier, J. P., J. C. Alliot, G. Labaune, et al., "Electromagnetic coupling on complex systems: Topological approach," Interaction Notes, Note 488, 1990.
7. Parmantier, J. P. and P. Degaugue, "Topology based modeling of very large systems," *Modern Radio Science*, J. Hamelin, Editor, 151–177, Oxford Univ. Press, Oxford, UK, 1996.
8. Parmantier, J. P., "Numerical coupling models for complex systems and results," *IEEE Trans. Electromagn. Compat.*, Vol. 46, No. 3, 359–367, 2004.
9. Parmantier, J. P., "First realistic simulation of effects of EM coupling in commercial aircraft wiring," *Computing & Control Engineering Journal*, Vol. 9, No. 2, 52–66, 1998.
10. Han, S. M., J. J. Bang, C. S. Huh, and J. S. Choi, "A PCB noise analysis regarding EMP penetration using an electromagnetic topology method," *Progress In Electromagnetics Research*, Vol. 122, 15–27, 2012.
11. Kirawanich, P., R. Gunda, N. S. Kranthi, J. C. Kroenung, and N. E. Islam, "Methodology for interference analysis using electromagnetic topology techniques," *Appl. Phys. Lett.*, Vol. 84, No. 15, 2949–2951, 2004.
12. Kirawanich, P., J. R. Wilson, N. E. Islam, and S. J. Yakura, "Minimizing crosstalks in unshielded twisted-pair cables by using electromagnetic topology techniques," *Progress In Electromagnetics Research*, Vol. 63, 125–140, 2006.

13. Xie, H., J. Wang, R. Fan, and Y. Liu, "Application of a spice model for multiconductor transmission lines in electromagnetic topology," *PIERS Proceedings*, 237–241, Cambridge, USA, July 2–6, 2008.
14. Xie, H., J. Wang, R. Fan, and Y. Liu, "Study of loss effect of transmission lines and validity of a SPICE model in electromagnetic topology," *Progress In Electromagnetics Research*, Vol. 90, 89–103, 2009.
15. Xie, H., J. Wang, D. Sun, R. Fan, and Y. Liu, "Analysis of EMP coupling to a device from a wire penetrating a cavity aperture using transient electromagnetic topology," *Journal of Electromagnetic Waves and Applications*, Vol. 23, Nos. 17–18, 2313–2322, 2009.
16. Xie, H., J. Wang, R. Fan, and Y. Liu, "SPICE models for prediction of disturbances induced by nonuniform fields on shielded cables," *IEEE Trans. Electromagn. Compat.*, Vol. 53, No. 1, 185–192, 2011.
17. Xie, H., J. Wang, D. Sun, and R. Fan, "Transient electromagnetic topology and its experimental validation," *Progress In Electromagnetics Research Letters*, Vol. 25, 185–195, 2011.
18. Tesche, F. M., M. V. Ianoz, and T. Karlsson, *EMC Analysis Methods and Computational Models*, Wiley, New York, 1997.
19. Vance, E. F., *Coupling to Shielded Cables*, John Wiley & Sons, New York, 1978.
20. Taylor C. D., R. S. Satterwhite, and C. W. Harrison, "The response of a terminated two-wire transmission line excited by a nonuniform electromagnetic field," *IEEE Trans. Antennas. Propag.*, Vol. 13, No. 6, 987–989, 1965.
21. Xie, H., J. Wang, R. Fan, and Y. Liu, "SPICE models to analyze radiated and conducted susceptibilities of shielded coaxial cables," *IEEE Trans. Electromagn. Compat.*, Vol. 52, No. 1, 215–222, 2010.
22. IEC 61000-2-9, "Description of HEMP environment-radiation disturbance-basic EMC publication," 1996.
23. Xie, H., J. Wang, R. Fan, and Y. Liu, "A hybrid FDTD-SPICE method for transmission lines excited by a nonuniform incident wave," *IEEE Trans. Electromagn. Compat.*, Vol. 51, No. 3, 811–817, 2009.
24. Neamen, D. A., *Semiconductor Physics and Devices: Basic Principles*, 3rd edition, McGraw-Hill, New York, 2003.